Synthesis, characterization and in vitro cytotoxicity of gold(III) dialkyl/diaryldithiocarbamato complexes

ARTICLE *in* RSC ADVANCES · SEPTEMBER 2015

Impact Factor: 3.84 · DOI: 10.1039/c5ra15123f

RSC Advances

PAPER

Cite this: *RSC Adv.*, 2015, **5**, 81599

Synthesis, characterization and *in vitro* cytotoxicity of gold(III) dialkyl/diaryldithiocarbamato complexes†

Muhammad Altaf,[a] Anvarhusein A. Isab,*[b] Ján Vančo,[c] Zdeněk Dvořák,[c] Zdeněk Trávníček*[c] and Helen Stoeckli-Evans[d]

Received 29th July 2015
Accepted 15th September 2015

DOI: 10.1039/c5ra15123f

www.rsc.org/advances

A series of six dialkyl/diaryldithiocarbamato (dtc) gold(III) complexes **1–6** of the composition $[Au(Me_2dtc)_2]Cl$ (**1**), $[Au(Me_2dtc)Cl_2]$ (**2**), $[Au(Et_2dtc)_2]Cl$ (**3**), $[Au(Et_2dtc)Cl_2]$ (**4**), $[Au(Bn_2dtc)_2]Cl$ (**5**), $[Au(Bn_2dtc)Cl_2]$ (**6**) (dtc = Dithiocarbamate, Me = Methyl, Et = Ethyl and Bn = Benzyl) was synthesised and characterized by elemental analysis, infrared and NMR spectroscopy, and single crystal X-ray analysis in the case of complexes **4** and **5**. The anticancer potential of the complexes was evaluated against MCF7, A2780 and A2780R human cancer cell lines as well as against a healthy MRC5 cell line. The most promising data were obtained for complex **4**. It showed similar cytotoxicity as cisplatin against A2780 cells ($EC_{50} \approx 9.5$ μM *vs.* $EC_{50} \approx 10$ μM), and significantly higher cytotoxicity as compared to cisplatin on A2780R and MCF7 cell lines, with $EC_{50} \approx 2.8$ μM *vs.* $EC_{50} \approx 21$ μM, and $EC_{50} \approx 2.2$ μM *vs.* $EC_{50} > 50$ μM, respectively. The interactions of the representative complexes **3** and **4** with a mixture of physiological levels of L-cysteine (Cys) and reduced L-glutathione (GSH) were also studied.

1. Introduction

Platinum-based metallo-drugs have been used effectively and widely for chemotherapy of cancers patients for many decades.[1–3] However, there are many concerns about the effectiveness of these drugs against different kinds of cancers.[4] The use of platinum(II) anticancer drugs is limited due to severe side effects such as neurotoxicity, ototoxicity, anaemia, nausea and the acquired as well as intrinsic resistances exhibited by cancer cell lines.[5,6] These undesirable and limiting factors of platinum(II) drugs are major impediments in their clinical use invariably against all kinds of cancers.[7] These adverse effects and limits of platinum-based drugs have prompted scientists to search for new alternative anticancer agents connected with other metals such as gold-based complexes. To date, gold(III) complexes have been synthesized and evaluated for their potential anticancer activity with lower toxicity and fewer side effects against a wide panel of cancer cell lines.[8–11]

Gold(III) adopts a square-planar geometry and is expected to imitate the structural and electronic properties of platinum(II); These structural and electronic similarities of gold(III) complexes have attracted scientists and researchers attention for their outstanding cytotoxic activity.[12–15] Recent studies have shown that several gold(III) complexes are highly cytotoxic against different tumor cells, including some cisplatin-resistant cancer cell lines.[16–18]

In this connection, a great interest in a new class of gold(III) complexes that contain dithiocarbamate ligands has been emerged as potential anticancer agents since 2000. Fregona and co-workers firstly prepared and characterized some novel gold(III) dithiocarbamate complexes containing *N*,*N*-dimethyldithiocarbamate and ethylsarcosinedithiocarbamate exhibiting the promising chemical and biological profile.[19] Similarly, significant inhibitory effect of dibromo(*N*,*N*-dimethyldithiocarbamato)gold(III) *in vivo* was reported against growth of MDA-MB-231 breast tumor cells (BTC).[20] Gold(I)-dithiocarbamato complexes, could inhibit the A549 (lung cancer), MCF7 (breast cancer), HeLa (cervical cancer) and chymotrypsin-like activity of purified 20S proteasome and 26S proteasome in human breast cancer MDA-MB-231 cells.[21–23] Gold(I) complexes with sulfur ligands were employed clinically in the treatment of rheumatoid arthritis displayed some potency against various tumors but a greater potential is found in their analogues featuring a

[a]*Centre of Research Excellence in Nanotechnology (CENT), King Fahd University of Petroleum and Minerals, Dhahran 31261, Saudi Arabia. E-mail: aisab@kfupm.edu.sa; zdenek.travnicek@upol.cz*

[b]*Department of Chemistry, King Fahd University of Petroleum and Minerals, Dhahran 31261, Saudi Arabia*

[c]*Regional Centre of Advanced Technologies and Materials, Division of Biologically Active Complexes and Molecular Magnets, Faculty of Science, Palacký University, 17. listopadu 12, CZ-771 46 Olomouc, Czech Republic*

[d]*Institute of Physics, University of Neuchâtel, rue Emile-Argand 11, CH-2000 Neuchâtel, Switzerland*

† Electronic supplementary information (ESI) available. CCDC 1403956 and 1403957. For ESI and crystallographic data in CIF or other electronic format see DOI: 10.1039/c5ra15123f

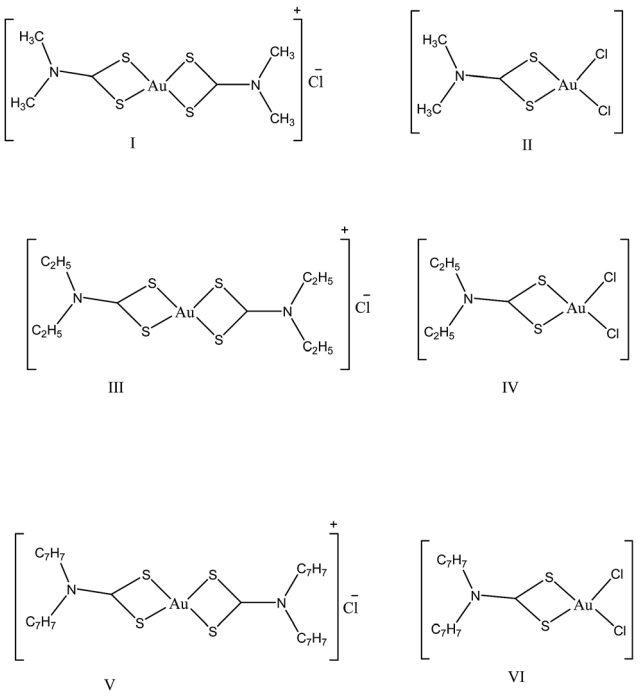

Scheme 1 Structural formulas of gold(III) complexes (**1–6**).

linear P–Au–S arrangement in which the thiolate ligand is derived from a biologically active thiol display high potency.[24] F.K. Keter *et al.* synthesized new gold complexes that contain sulfur donor ligands (pyrazolyldithiocarbamate or 3,5-dimethylpyrazolyldithiocarbamate or indazolyldithiocarbamate) and found all complexes active against human cervical epithelial cancer cells (HeLa).[25]

This article follows our previous investigation of mixed ligand Au(I) complexes that contain dialkyl/diaryldithiocarbamate and phosphine ligands with excellent *in vitro* cytotoxicity against a panel of human cancer cells.[22,26,27] Here, we have decided to use Au(III) acceptor and dialkyl/diaryldithiocarbamato and chlorido ligands. As we know that coordination and electronic features of the Au(I) center are different from Au(III) center. Herein, we report the synthesis, characterization, *in vitro* cytotoxicity of Au(III) complexes (Scheme 1) in normal human foetal lung cells (MRC5) and three different human cancer cell lines including breast (MCF7) and ovarian (A2780, A2780R), and cisplatin as control. The gold(III) complex **4** was also evaluated for its ability of interactions with L-cysteine (Cys) and reduced L-glutathione (GSH) by mass spectrometry.

2. Experimental

2.1. Materials and methods

Sodium tetrachloroaurate(III) dihydrate, sodium dimethyldithiocarbamate monohydrate, sodium diethyldithiocarbamate trihydrate and sodium dibenzyldithiocarbamate hydrate were purchased from Sigma-Aldrich Co. St. Louis, Missouri, United States. All solvents including ethanol, and dichloromethane were purchased from Merck Darmstadt, Germany and used without further purification. All reactions were carried out under ambient conditions.

Elemental analyses of gold(III) complexes **1–6** were performed on Perkin-Elmer Series 11 (CHNS/O), Analyzer 2400. The solid state FTIR spectra of free ligands and their corresponding gold(I) complexes were recorded on a Perkin-Elmer FTIR 180 spectrophotometer or NICOLET 6700 FTIR using potassium bromide (KBr) pellets over the range 4000–400 cm^{-1}. The electronic (UV/Vis) spectra were collected on a LAMBDA 40 spectrometer (Perkin-Elmer, USA).

^{1}H and ^{13}C NMR spectra were recorded on a LAMBDA 500 spectrophotometer operating at 500.01, 125.65, and 200.0 MHz, respectively; corresponding to a magnetic field of 11.74 T. Tetramethylsilane (TMS) was used as an internal standard for ^{1}H and ^{13}C. The ^{13}C NMR spectra were obtained with ^{1}H broadband decoupling, and the spectral conditions were: 32k data points, 0.967 s acquisition time, 1.00 s pulse delay and 45° pulse angle.

Electrospray-ionization (ESI) mass spectra of methanol solutions of the complexes were recorded on an LCQ Fleet Ion-Trap mass spectrometer using both the positive (ESI+) and negative (ESI−) mode of electrospray ionization (Thermo Scientific, USA).

2.2. Synthesis

2.2.1. Synthesis of [Au(Me$_2$dtc)$_2$]Cl (1). [Au(Me$_2$dtc)$_2$]Cl (**1**) was synthesized according to our previously reported procedure with minor modifications. $NaAuCl_4 \cdot 2H_2O$, 0.5 mM (200 mg) and sodium dimethyldithiocarbamate dihydrate 1.0 mM (144 mg) in 20 mL of water and ethanol (1 : 1) were refluxed for 1 h. The complex appeared as bright yellow precipitate in the reaction medium. The precipitate was collected, washed with fresh distilled water (3 × 10 mL) and dried at room temperature for 24 h. The product appeared as bright yellow lumps. Yield: 93.09% (219.98 mg). FT-IR (KBr, ν_{max}, cm^{-1}): 2916 (w); 1576 (m), 1480 (s), 1243 (m), 1161 (w), 1093 (m), 961 (m), 925 (w), 555 (m), 473 (m). ^{1}H NMR (500 MHz, DMSO-d_6): δ = 3.37 (12H, s, 4 × CH_3). ^{13}C NMR (125.1 MHz, DMSO-d_6): δ = 35.15 (CH_3), 186.86 (NC═S). Anal. calc. for $C_6H_{12}ClN_2S_4Au$ (472.85): C, 15.24; H, 2.56; N, 5.92; S, 27.12%. Found: C, 15.31; H, 2.58; N, 5.95; S, 27.15%.

2.2.2. Synthesis of [Au(Me$_2$dtc)Cl$_2$] (2). [Au(Me$_2$dtc)Cl$_2$] (**2**) was synthesized according to the procedure as mentioned above for complex **1** with minor modifications.[26–29] $NaAuCl_4 \cdot 2H_2O$, 0.5 mM (200 mg) and sodium dimethyldithiocarbamate dihydrate 0.5 mM (72 mg) in 20 mL of water and ethanol (1 : 1) were refluxed for 1 h. The complex appeared as yellow precipitate in the reaction medium. The precipitate was collected, washed with fresh distilled water (3 × 10 mL) and dried at RT for 24 h. The product appeared as yellow crystalline powder. Yield: 86.87% (166.87 mg). FT-IR (KBr, ν_{max}, cm^{-1}): 2923 (w); 1571 (s), 1481 (m), 1241 (m), 1160 (w), 1095 (m), 966 (m), 920 (w), 550 (m), 472 (m). ^{1}H NMR (500 MHz, DMSO-d_6): δ = 3.35 (6H, s, 2 × CH_3). ^{13}C NMR (125.1 MHz, DMSO-d_6): δ = 34.15 (CH_3), 193.89

(NC═S). Anal. calc. for $C_3H_6Cl_2NS_2Au$ (388.10): C, 9.28; H, 1.56; N, 3.61; S, 16.52%. Found: C, 9.17; H, 1.58; N, 3.59; S, 16.55%.

2.2.3. Synthesis of [Au(Et$_2$dtc)$_2$]Cl (3). [Au(Et$_2$dtc)$_2$]Cl (**3**) was synthesized according to the procedure as mentioned above for complex **1** with minor modifications. $NaAuCl_4 \cdot 2H_2O$, 0.5 mM (200 mg) and sodium diethyldithiocarbamate trihydrate 1.0 mM (226 mg) in 20 mL of water and ethanol (1 : 1) were refluxed for 1 h. The complex appeared as light brown lumps in the reaction medium. The solid product was collected, washed with fresh distilled water (3 × 10 mL) and dried at RT for 24 h. The product appeared as light brown lumps. Yield: 85.55% (226.13 mg). FT-IR (KBr, ν_{max}, cm^{-1}): 2977 (w), 2930 (w), 1550 (m), 1483 (s), 1285 (m), 1158 (w), 1089 (m), 998 (m), 907 (w), 550 (s), 480 (m). ^{1}H NMR (500 MHz, DMSO-d$_6$): δ = 1.29 (12H, d, 4 × CH_3), 3.75 (8H, d, 4 × CH_2). ^{13}C NMR (125.1 MHz, DMSO-d$_6$): δ = 12.15 (CH_3), 46.60 (CH_2), 193.87 (NC═S). Anal. calc. for $C_{10}H_{20}ClN_2S_4Au$ (528.96): C, 22.71; H, 3.81; N, 5.30; S, 24.25%. Found: C, 22.63; H, 3.85; N, 5.26; S, 24.33%.

2.2.4. Synthesis of [Au(Et$_2$dtc)Cl$_2$] (4). [Au(Et$_2$dtc)Cl$_2$] (**4**) was synthesized according to our previously reported procedure with minor modifications.[26–29] $NaAuCl_4 \cdot 2H_2O$, 0.5 mM (200 mg) and sodium diethyldithiocarbamate trihydrate 0.5 mM (113 mg) in 20 mL of water and ethanol (1 : 1) were refluxed for 1 h. The complex appeared as light yellow precipitate in the reaction medium. The precipitate was collected, washed with fresh distilled water (3 × 10 mL) and dried at RT for 24 h. The product appeared as light yellow semi crystalline cluster. Yield: 90.09% (187.27 mg). FT-IR (KBr, ν_{max}, cm^{-1}): 2970 (w), 2921 (w), 1556 (m), 1482 (s), 1280 (m), 1155 (w), 1078 (m), 991 (m), 909 (w), 550 (s), 481 (m). ^{1}H NMR (500 MHz, DMSO-d$_6$): δ = 1.28 (6H, d, 2 × CH_3), 3.75 (4H, d, 2 × CH_2). ^{13}C NMR (125.1 MHz, DMSO-d$_6$): δ = 12.13 (CH_3), 46.62 (CH_2), 193.88 (NC═S). Anal. calc. for $C_5H_{10}Cl_2NS_2Au$ (416.15): C, 14.43; H, 2.42; N, 3.37; S, 15.41%. Found: C, 14.33; H, 2.47; N, 3.31; S, 15.47%.

2.2.5. Synthesis of [Au(Bn$_2$dtc)$_2$]Cl (5). [Au(Bn$_2$dtc)$_2$]Cl (**5**) was synthesized according to the procedure as mentioned above for complex **3** with minor modifications. $NaAuCl_4 \cdot 2H_2O$, 0.5 mM (200 mg) and sodium dibenzyldithiocarbamate hydrate 1.0 mM (296 mg) in 20 mL of methanol and water (9 : 1) were refluxed for 1 h. The complex appeared as dark brown precipitate in the reaction medium. The precipitate was collected, washed with fresh distilled water (3 × 10 mL) and dried at RT for 24 h. The product appeared as dark brown lumps. Yield: 88.51% (343.9 mg). FT-IR (KBr, ν_{max}, cm^{-1}): 3035 (w), 2993, 2916 (m), 1534 (s), 1491 (s), 1352 (m), 1227 (s), 1126 (m), 1071 (m), 977 (s), 800 (m), 533 (s), 468 (m). ^{1}H NMR (500 MHz, DMSO-d$_6$): δ = 5.03 (8H, s, 4 × CH_2), 7.37 (20H, m, 4 × C_6H_5). ^{13}C NMR (125.1 MHz, DMSO-d$_6$): δ = 55.08 (CH_2), 132.55 (C_6H_5), 199.18 (NC═S). Anal. calc. for $C_{30}H_{28}ClN_2S_4Au$ (777.23): C, 46.36; H, 3.63; N, 3.60; S, 16.50%. Found: C, 46.30; H, 3.64; N, 3.68; S, 16.59%.

2.2.6. Synthesis of [Au(Bn$_2$dtc)Cl$_2$] (6). [Au(Bn$_2$dtc)Cl$_2$] (**6**) was synthesized according to the procedure as mentioned above for complex **4** with minor modifications. $NaAuCl_4 \cdot 2H_2O$, 0.5 mM (200 mg) and sodium dibenzyldithiocarbamate hydrate 0.5 mM (148 mg) in 20 mL of methanol and water (9 : 1) were refluxed for 1 h. The complex appeared as yellowish green precipitate in the reaction medium. The precipitate was collected, washed with fresh distilled water (3 × 10 mL) and dried at RT for 24 h. The product appeared as yellowish green powder. Yield: 95.01% (256.6 mg). FT-IR (KBr, ν_{max}, cm^{-1}): 3034 (w), 2990, 2923 (m), 1540 (s), 1495 (s), 1355 (m), 1229 (s), 1129 (m), 1079 (m), 979 (s), 808 (m), 537 (s), 458 (m). ^{1}H NMR (500 MHz, DMSO-d$_6$): δ = 5.01 (4H, s, 2 × CH_2), 7.36 (10H, m, 2 × C_6H_5). ^{13}C NMR (125.1 MHz, DMSO-d$_6$): δ = 55.09 (CH_2), 132.54 (C_6H_5), 199.16 (NC═S). Anal. calc. for $C_{15}H_{14}Cl_2NS_2Au$ (540.28): C, 33.35; H, 2.61; N, 2.59; S, 11.87%. Found: C, 33.43; H, 2.70; N, 2.53; S, 11.91%.

2.3. X-ray structure determination

Suitable crystals of complex **4** and **5** were obtained as orange rods and yellow plates by recrystallization of final products in mixture of chloroform and methanol (1 : 1) solution. The intensity data were collected at 173 K (−100 °C) on a Stoe Mark II-Image Plate Diffraction System[30] equipped with a two-circle goniometer and using MoKα graphite monochromated radiation (λ = 0.71073 Å). The structure was solved by direct methods with SHELXS-2014.[31] The refinement and all further calculations were carried out with SHELXL-2014.[32] For complex **4**, the C-bound H-atoms were included in calculated positions and treated as riding atoms: C–H = 0.99 and 0.98 Å for CH_2, and CH_3, respectively, with U_{iso}(H) = 1.5U_{eq}(C-methyl) and = 1.2U_{eq}(C) for other H-atoms. For complex **5**, the C-bound

Table 1 Crystal data and structure refinement details for complexes **4** and **5**

Complex	**4**	**5**
CCDC deposit no.	1403956	1403957
Chemical formula	$[C_5H_{10}NS_2AuCl_2]$	$[(C_{15}H_{14}NS_2)_2Au]^+ \cdot (AuCl_2)^-$
Molecular weight	416.13	1009.62
Crystal system, space group	Monoclinic, $P2_1/n$	Monoclinic, $P2_1/c$
Temperature (K)	173	173
a, b, c (Å)	17.2433 (8), 7.0535 (3), 17.2503 (10)	10.0213 (12), 18.6050 (17), 9.1040 (12)
β (°)	97.718 (4)	109.36 (1)
V (Å^3)	2079.07 (18)	1601.4 (3)
Z	8	2
Radiation type	Mo Kα	Mo Kα
μ (mm^{-1})	15.01	9.60
Crystal size (mm)	0.40 × 0.35 × 0.30	0.45 × 0.17 × 0.10
T_{min}, T_{max}	0.454, 1.000	0.401, 1.000
No. of measured, independent and observed [$I > 2\sigma(I)$] reflections	24 350, 3929, 3519	10 925, 3028, 1874
R_{int}	0.084	0.042
(sin $\theta/\lambda)_{max}$ (Å^{-1})	0.609	0.610
$R[F^2 > 2\sigma(F^2)]$, w$R(F^2)$, S	0.022, 0.048, 0.92	0.019, 0.040, 0.77
No. of reflections	3929	3028
No. of parameters	205	185
Largest diff. peak and hole (e Å^{-3})	1.25, −1.94	1.03, −0.74
$\Delta\rho_{max}$, $\Delta\rho_{min}$ (e Å^{-3})		

H-atoms were included in calculated positions and treated as riding atoms: C–H = 0.95–0.99 Å with $U_{iso}(H) = 1.2U_{eq}(C)$. The non-H atoms were refined anisotropically, using weighted full-matrix least-squares on F^2 Table 1. A semi-empirical absorption correction was applied using the MULscanABS routine in PLATON.[33] The summary of crystallographic data and structure refinement of complexes **4** and **5** is given in Table 1.

2.4. Cell cultures and *in vitro* cytotoxicity

Human breast adenocarcinoma cells (MCF7; ECACC no. 86012803), human ovarian carcinoma cells (A2780; ECACC no. 93112519), cisplatin-resistant human ovarian carcinoma cells (A2780R; ECACC no. 93112517) and human foetal lung cells (MRC5; ECACC no. 84101801) were purchased from European Collection of Cell Cultures (ECACC). The cells were cultured according to the ECACC instructions and they were maintained at 37 °C and 5% CO_2 in a humidified incubator. The cells were treated with the tested complexes, and cisplatin, respectively, for 24 h, using multiwell culture plates of 96 wells. In parallel, the cells were treated with vehicle (DMF; 0.1%, v/v) and Triton X-100 (1%, v/v) to assess the minimal (*i.e.* the positive control), and maximal (*i.e.* the negative control) cell damage, respectively. The MTT assay was performed spectrophotometrically at 540 nm (TECAN, Schoeller Instruments LLC).

2.5. Mass spectrometry study of interactions of complexes 3 and 4 with L-cysteine and reduced glutathione

The interaction experiments between the selected representative complexes **3** and **4**, and the mixture of physiological levels of L-cysteine (Cys) and reduced L-glutathione (GSH) were performed on a Thermo Scientific LTQ Fleet Ion-Trap mass spectrometer, using the positive ionization mode. The reaction system contained the physiological concentrations of L-cysteine (290 μM) and reduced glutathione (6 μM)[54] and the tested complex (10 μM) in the methanol : water (1 : 1, v/v) mixture. The reference system was comprised of the solution of complex (10 μM) in the methanol : water (1 : 1, v/v) mixture. The flow injection analysis (FIA) method was used to introduce the reaction system (10 μL spikes) into the mass spectrometer, while the mixture of acetonitrile : water (9 : 1, v/v) was used as a mobile phase. The electro-spray ionization (ESI) source was set up as follows: source voltage was 4.9 kV, the vaporizer temperature was 160 °C, the capillary temperature was 275 °C, the sheath gas flow rate was 20 L min^{-1}, and auxiliary gas flow rate was 5 L min^{-1}. The system was calibrated according to the manufacturer specifications and no further tuning was needed.

3. Results and discussion

3.1. Characterization by FT-IR

Gold(III) dithiocarbamate complexes **1–6** were identified *via* the presence of certain absorbance peaks primarily ν(C–N) and ν(C–S). The infrared region 1480–1550 cm^{-1} is mostly related with the R_2N–CSS 'thioureide' band in the IR spectra of dithiocarbamate complexes which defines the carbon–nitrogen bond order between a single bond at 1250–1350 cm^{-1} and a double bond at 1640–1690 cm^{-1}.[34]

The thioureide band, ν(C–N) was detected at 1481, 1480, 1482, 1483, 1495 and 1491 cm^{-1} in complexes **1–6** respectively. Such frequency absorption bands lie in between those associated with single C–N and double C=N bonds, hence the partial double bond character of 'thioureide' bond was confirmed for all gold(I) complexes.[35] The presence of strong absorption band in the range of 1480–1550 in FTIR spectra clearly indicates the formation of dithiocarbamato gold(III) complexes.[36,37] Similarly, C=S stretching with medium intensity around 1070 and 970 cm^{-1} for complexes **1–6** is an additional evidence of the formation of target molecules. The common bands for sp^3, sp^2 and sp hybridized C–H stretches were observed within 2995–2915 cm^{-1} and above 3000 cm^{-1} respectively. These absorption bands are comparable to free sodium salt of diethyldithiocarbamate ligands.[38]

3.2. Characterization by NMR

The ^{1}H NMR chemical shifts of all six complexes are given in the Section 2.2. Synthesis. Small downfield and upfield shifts for proton(s) of the coordinated dimethyl dithiocarbamate, diethyl dithiocarbamate and dibenzyldithiocarbamate have been seen in gold(III) complexes **1–6** in comparison to free dialkyl/diaryldithiocarbamate ligands.[22,26,29,39–43]

The ^{13}C NMR spectra of complexes **1**, **2** and **3–6** showed two and three resonances respectively (given in synthesis part of Experimental Section). There is an up-field chemical shift of NC=S carbon of coordinated dialkyldithiocarbamate with respect to free dialkyl/diaryldithiocarbamate ligands for all gold(III) complexes. The ^{13}C chemical shifts of NC=S carbon of bonded dimethyl thiocarbamate, diethyl thiocarbamate and dibenzyl thiocarbamate are observed in the range 186–200 ppm in our synthesized complexes **1–6**.[22,26,29,39–43]

3.3. X-ray crystallography

X-ray structure and crystal packing of complex **4** is shown in Fig. 1 and 2. The complex **5** crystallized with two independent molecules per asymmetric unit. The crystal structure contains two independent molecules in which Au(III) centre is tetra-coordinated and surrounded by two chlorine atoms and both sulfur atoms of the diethyldithiocarbamate ligand in a *cis* position. The geometry around gold(III) ions is square planar (Cl–Au–Cl angle is 94.17(10) and 94.36(11)° for molecule 1 and molecule 2 respectively), although somehow distorted as a consequence of the restricting chelate angle of the dithiocarbamate ligand (S–Au–S 75.87(10) and 75.57(11)° for molecule 1, and molecule 2, respectively). This angle lies within the range found in a total of 76 entries in 41 crystal structures containing the fragment [Au(μ-S_2CN)], which vary from 65.71(5) to 78.6(3)° (mean value of 75.87°).[44,45]

The Au_1–S_2 and Au_2–S_3 bond distances 2.294(2) and 2.293(2) Å are almost same in molecule 1 and molecule 2 respectively. Similarly Au_1–S_1 and Au_2–S_4 bond distances 2.310(3) and 2.312(3) Å are also very close in molecule 1, and molecule 2, respectively. The Au–Cl average bond lengths of 2.324(3) and

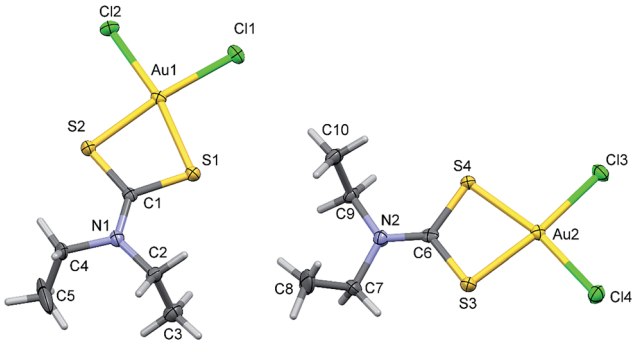

Fig. 1 A view of the two crystallographically independent molecules of complex **4**, together with the atom labelling scheme. The displacement ellipsoids are drawn at the 50% probability level.

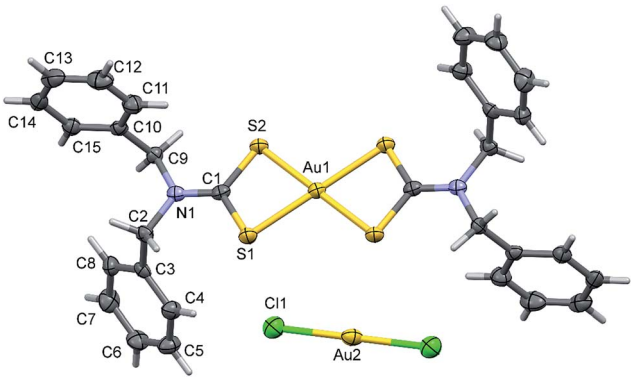

Fig. 3 A view of the molecular structure of complex **5**, together with the atom labelling scheme. The displacement ellipsoids are drawn at the 50% probability level. The unlabelled atoms are generated by inversion symmetry [symmetry codes for Au_1: $-x, -y, -z$, and for Au_2: $-x+1, -y, -z$].

2.326(3) Å for molecule 1, and molecule 2, respectively, is slightly long for a gold(III) complex. This is due to the strong trans influence of the S donor ligands and is of the same order as the Au–Cl bond distances found in the related dithiocarbamate Au(III) complexes or in other complexes containing the fragment $[AuCl_2(\mu\text{-SCS})]$.[46–48]

The molecular structure of complex **5** is shown in Fig. 3 and 4. In ionic complex **5**, one gold atom coordinates with two structurally equivalent dibenzyldithiocarmate ligand molecules in the *S*,*S*′-bidentate mode, thus forming the centrosymmetric $[Au(Bn_2dtc)_2]^+$ cation. The second Au(I) atom in the centrosymmetric $[AuCl_2]^-$, is surrounded by two chloride anions. In one coordination sphere, gold(III) forms square-planar tetragonal chromophores: $[AuS_4]$ (low spin intra-orbital dsp^2 hybrid state of the central gold(III) atom). Whereas, in second coordination sphere, gold(I) attains a linear geometry (Table 2).

The S_1–Au_1–S_2, and S_2–Au_1–S_1^i bond angles in this centrosymmetric $[Au(Bn_2dtc)_2]^+$ cation, are 75.44(4), and 104.56(4)° respectively. The Au_1–S_1 and Au_1–S_2 bond distances are 2.3396(10) and 2.3343(10) Å respectively. The Au–S bond length in **2** is nearly identical with the mean value of 2.3038 Å found in Au(III) complexes that contain dithiocarbamate ligands, in which the Au–S bond distances vary from 2.287(3) Å in $[AuCl_2\{\mu\text{-}S_2CN(EtOH)_2\}]$ to 2.319(2) Å in $[AuBr_2\{\mu\text{-}S_2CN(Me)(CH_2CO_2Et)\}]$. It also compares well with those observed in the $[AuCl_2(\mu\text{-SCS})]$ complexes.[49–52]

3.4. *In vitro* cytotoxicity

Normal human foetal lung cells (MRC5) and three different human cancer cell lines including breast (MCF7) and ovarian (A2780, A2780R) were used as experimental models for evaluation of *in vitro* cytotoxicity of the prepared complexes **1–6**, see Table 3. The cells were incubated with the studied complexes for 24 h and the viability was assessed by a conventional MTT test. The cytotoxicity of complexes **1**, **2**, **5** and **6** was lower or comparable to that by cisplatin, regardless the particular cell line. Complex **3** displayed similar toxicity as cisplatin in both ovarian cancer cells A2780 and their cisplatin-resistant variant A2780R. On the other hand, complex **3** displayed in order of magnitude higher cytotoxicity against breast cancer cells MCF7 as compared to cisplatin ($EC_{50} \approx 3.9$ μM *vs.* $EC_{50} > 50$ μM), but

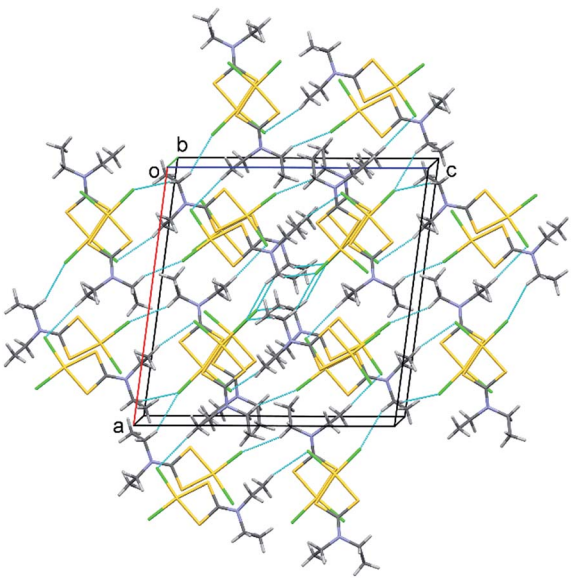

Fig. 2 The crystal packing of complex **4**, as viewed along the *a* axis.

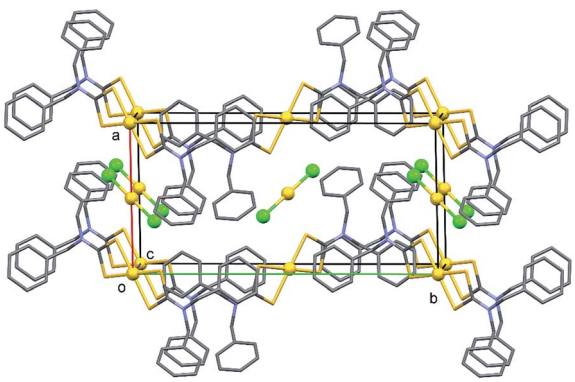

Fig. 4 The crystal packing of complex **5**, as viewed along the *c* axis.

Table 2 Selected bond lengths and bond angles of complexes **4** and **5**

Bond lengths (Å)		Bond angles (°)	
Complex 4			
Molecule 1			
$Au_1–S_2$	2.294(2)	$S_2–Au_1–S_1$	75.87(10)
$Au_1–S_1$	2.310(3)	$S_2–Au_1–Cl_1$	172.47(11)
$Au_1–Cl_1$	2.323(3)	$S_1–Au_1–Cl_1$	96.71(10)
$Au_1–Cl_2$	2.325(3)	$S_2–Au_1–Cl_2$	93.25(11)
		$S_1–Au_1–Cl_2$	169.11(12)
		$Cl_1–Au_1–Cl_2$	94.17(10)
Molecule 2			
$Au_2–S_3$	2.293(2)	$S_3–Au_2–S_4$	75.57(11)
$Au_2–S_4$	2.312(3)	$S_3–Au_2–Cl_4$	93.52(11)
$Au_2–Cl_4$	2.326(3)	$S_4–Au_2–Cl_4$	169.07(12)
$Au_2–Cl_3$	2.326(3)	$S_3–Au_2–Cl_3$	171.81(11)
		$S_4–Au_2–Cl_3$	96.57(10)
		$Cl_4–Au_2–Cl_3$	94.36(11)
Complex 5			
$Au_1–S_2$	2.3343(10)	$S_2–Au_1–S_2^i$	180.0
$Au_1–S_2^i$	2.3343(10)	$S_2–Au_1–S_1^i$	104.56(4)
$Au_1–S_1^i$	2.3396(10)	$S_2^i–Au_1–S_1^i$	75.44(4)
$Au_1–S_1$	2.3396(10)	$S_2–Au_1–S_1$	75.44(4)

still keeping low toxicity against normal MRC5 cells ($EC_{50} \approx$ 19.7 μM). The most promising data were obtained for complex **4**. While it showed similar cytotoxicity as cisplatin against A2780 cells ($EC_{50} \approx$ 9.5 μM *vs.* $EC_{50} \approx$ 10.0 μM), its cytotoxicity in cisplatin-resistant A2780R cells was drastically increased as compared to cisplatin ($EC_{50} \approx$ 2.8 μM *vs.* $EC_{50} \approx$ 21.0 μM). Moreover, complex **4** was much more toxic against breast cancer cells MCF7, as compared to cisplatin ($EC_{50} \approx$ 2.2 μM *vs.* $EC_{50} >$ 50 μM), showing moderate toxicity against healthy MRC5 cells.

3.5. Interactions of complexes 3 and 4 with sulphur-containing biomolecules analysed by mass spectrometry

It is a known fact, that gold(III) complexes bind to sulfanyl-containing substances, such as amino acid L-cysteine (Cys) or small proteins, such as reduced L-glutathione (GSH), and high molecular weight proteins (*e.g.* albumin or globulins[53]), in the biologically relevant environments, such as blood or serum. The complexes formed by these interactions can be considered as transport intermediates and/or detoxication end-products in some cases. These processes are connected with changes in oxidation states and exchanges of ligands of the original complexes. In this work, we strived to uncover interaction potential of the selected complexes **3** and **4** (applied in the concentration of 10 μM, roughly corresponding to the determined EC_{50} values), in biologically relevant conditions using a mixture of Cys (at the 290 μM concentration) and GSH (at the 6 μM concentration).[54] The complexes were chosen in connection with the fact that they contain the diethyldithiocarbamate moiety, however, on the other side each of them represents structurally different type of the complexes presented in this study, and moreover, they are also the most cytotoxic ones against the MCF7 cell line.

Table 3 *In vitro* cytotoxicity of the complexes **1–6** and cisplatin given as $EC_{50} \pm$ S.D. in μM

Complex	A2780	A2780R	MCF7	MRC5
1	16.8 ± 2,0	27.5 ± 2.3	19.4 ± 3.6	28.0 ± 1.4
2	7.3 ± 0.8	40.5 ± 4.2	21.5 ± 3.1	27.1 ± 2.9
3	6.3 ± 2.1	29.8 ± 5.8	3.9 ± 2.3	19.7 ± 6.4
4	9.5 ± 0.3	2.8 ± 0.1	2.2 ± 0.9	20.3 ± 0.8
5	27.1 ± 5.0	35.9 ± 2.3	>50	>50
6	25.1 ± 1.8	41.9 ± 1.2	>50	>50
Cisplatin	10.0 ± 1.6	21.0 ± 2.1	>50	>50

Based on the results of the mass spectrometry experiments, we may confirm that both the complexes **3** and **4** interact with the applied sulphur-containing substances in time-dependent manner by the ligand-exchange mechanism connected with the substitution of one diethyldithiocarbamato ligand for one cysteine and/or cystine (CysCys) molecule(s). (Note: CysCys represents an oxidation product of L-cysteine). This mechanism may be supported by the presence of the peaks at 465.03 *m*/*z* (for **4**), 613.11 *m*/*z* (for **3** and **4**), 704.90 *m*/*z* (for **4**), 852.86 *m*/*z* (for **3** and **4**), and 874.83 *m*/*z* (for **3** and **4**), corresponding to the species of $[Au(Et_2dtc) + Cys]^+$, $[Au(Et_2dtc)_2 + Cys]^+$, $[Au(Et_2dtc) + Cys + CysCys]^+$, $[Au(Et_2dtc)_2 + Cys + CysCys]^+$, and $[Au(Et_2dtc)_2 + Cys + CysCys + Na]^+$ species, respectively (see Fig. 5, and Fig. S1 in ESI†).

Moreover, the performed experiments were also useful to reveal the solvolytic behaviour of the complexes, because the peaks at 116.10 *m*/*z* and 493.08 *m*/*z* revealed in the ESI + mass spectra of complexes **3** and **4**, and they may be associated with the formation of the identical species of $[Et_2N–C{=}S]^+$, and $[Au(Et_2dtc)_2]^+$, respectively, see Fig. 6. In addition to that, the peak at 267.03 *m*/*z* was observed in the ESI-mass spectra of **3** and **4**, and it may be related to the presence of the $[AuCl_2]^-$ species. These findings motivated us to use mass spectrometry to thorough study of all the complexes with the aim to find out the stability of them in methanol. Surprisingly, we have found that the dissolution of complexes **1**, **3** and **5**, having the general formula $[Au(dtc)_2]Cl$, as well as complexes **2**, **4** and **6**, with the composition of $[Au(dtc)Cl_2]$, in methanol led to the formation of the $[Au(dtc)_2]^+$ and $[AuCl_2]^-$ species for **1**, **3** and **5**, and the $[Au(dtc)_2]^+$, $[AuCl_2]^-$ and $[AuCl_4]^-$ species for **2**, **4** and **6**, as demonstrated in Fig. 7 for the representative complexes **1** and **2**. The reduction of Au(III) to Au(I), as seen from the $[AuCl_2]^-$ species depicted in Fig. 7, is compensated by oxidation of Me_2dtc to $[Me_2N–CS–S–S–SC–NMe_2]^-$.

The above described findings may logically lead to the conclusion that mainly the $[Au(dtc)_2]^+$ species are responsible for interactions with sulphur-containing biomolecules (*i.e.* with Cys and GSH), and moreover, that these cationic species are also responsible for biological response, *i.e.* for the cytotoxicity of the complexes **1–6**. The above said may be supported by cytotoxicity data given in Table 3, because the EC_{50} values between **1** and **2**, between **3** and **4**, and between **5** and **6**, are close to each other, except for the complex **3** in the case of the A2780R cell line, however, this discrepancy may be explained

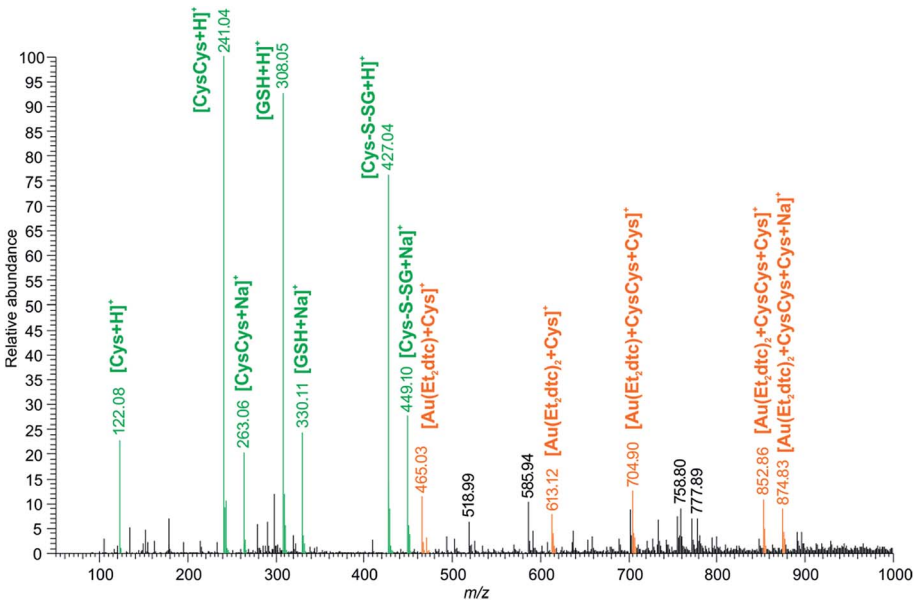

Fig. 5 The results of mass spectrometry study of interactions of complex **4** with physiological levels of L-cysteine (Cys) and reduced L-glutathione (GSH). Cystine (Cys–Cys) represents an oxidation product of cysteine. The peaks of Cys and GSH and their oxidized products are highlighted in green colour, while the peaks corresponding to the interaction adducts of complex **4** are given in orange colour.

by a possible biological impact of other species presented in the medium used for biological testing. Overall, it may be emphasized that the $[Au(dtc)Cl_2]$ complexes (**2**, **4** and **6**) decompose most probably to two dominant species, *i.e.* to $[Au(dtc)_2]^+$ and $[AuCl_4]^-$. This may be also supported by solution UV/Vis spectra of complexes **3** and **4** (measured in MeOH and DMF), (see Fig. S2 and S3 in ESI†), from which can be seen that the positions of maxima of the d–d transitions for complex **3** and **4** are nearly identical both in the MeOH and DMF solution.

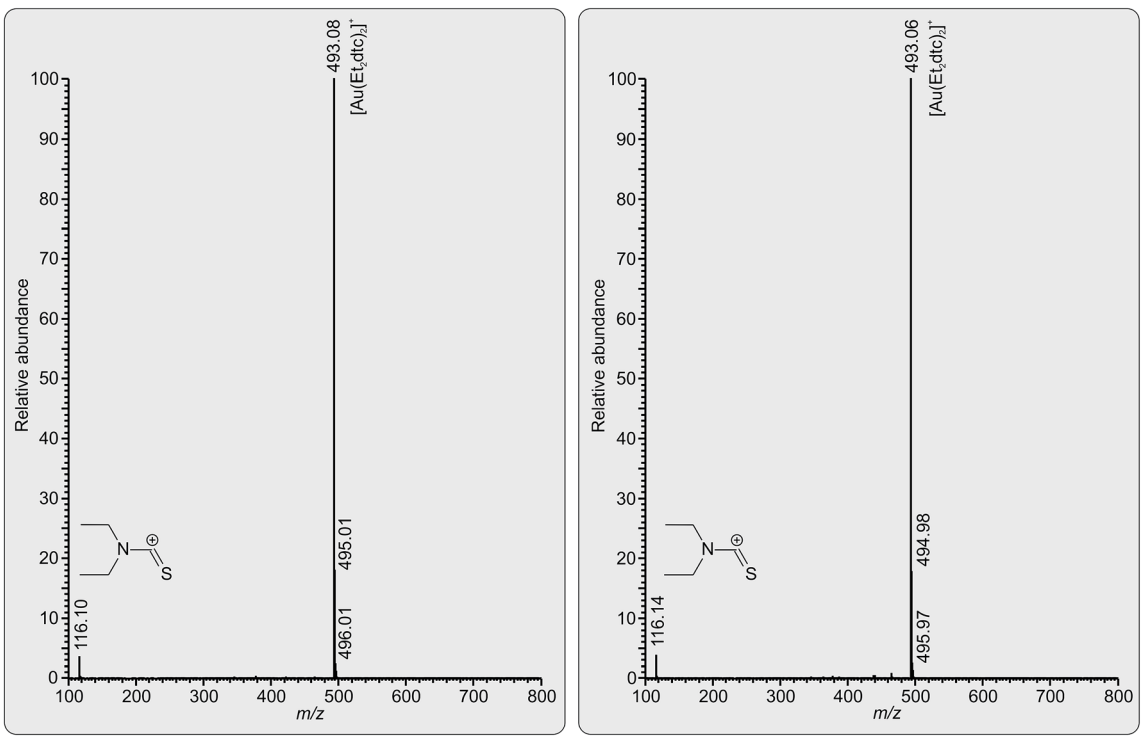

Fig. 6 The comparison of ESI + mass spectra of complexes **3** (left) and **4** (right) measured in methanol solutions, showing the presence of the peaks corresponding to the same cationic species $[Et_2N{-}C{=}S]^+$ and $[Au(Et_2dtc)_2]^+$.

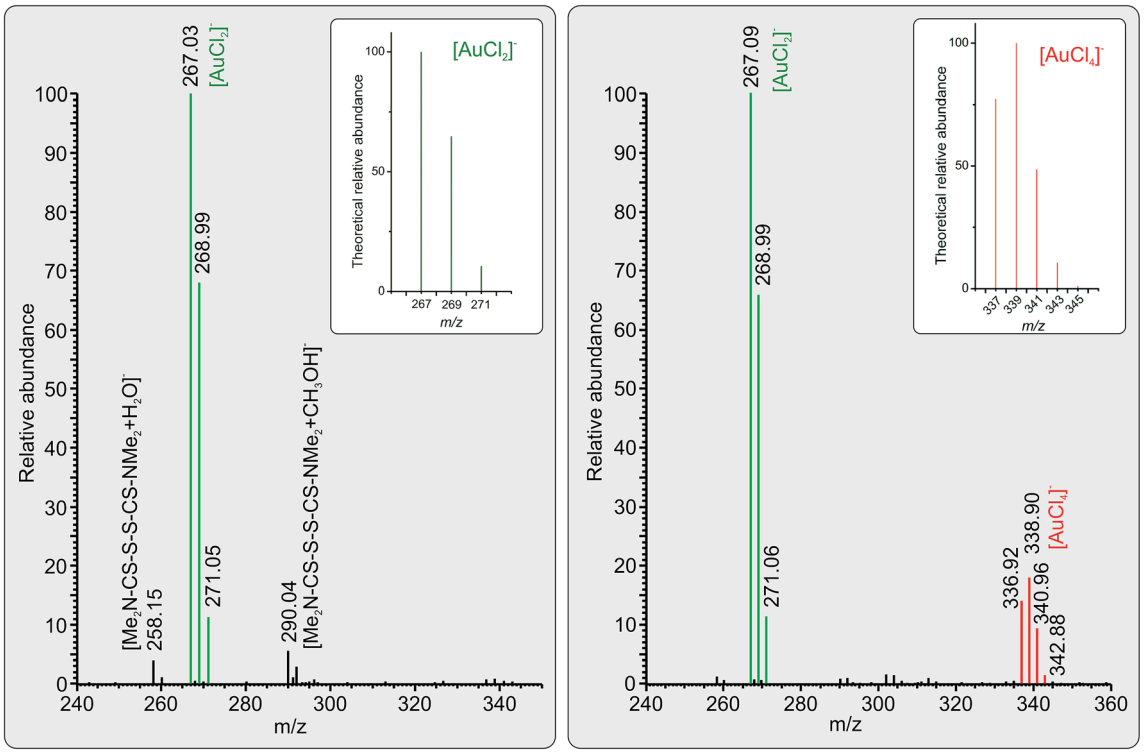

Fig. 7 The comparison of ESI-mass spectra of complexes **1** (left) and **2** (right) in methanol solutions, showing the presence of $[AuCl_2]^-$ and $[AuCl_4]^-$ species as well as species responding to oxidation of the dimethyldithiocarbamate moiety. The insets show the isotopic distributions for the corresponding species.

4. Conclusions

The synthesis and characterization of dialky/diaryldithiocarbamato gold(III) complexes **1–6** are reported. The *in vitro* cytotoxicity of the complexes has been evaluated against MCF7, A2780 and cisplatin-resistant A2780R human cancer cell lines as well as against healthy MRC5 cell line. The best cytotoxicity has been achieved for complex **4** against A2780R and MCF7, with the EC_{50} values of 2.8(1), and 2.2(9) μM, respectively, and with moderate toxicity on healthy MRC5 cell line (EC_{50} = 20.3(8) μM). Moreover, the results of interaction experiments of the representative complexes **3** and **4** with the mixture of physiological levels of L-cysteine (Cys) and reduced L-glutathione (GSH) revealed that the complexes interact with the applied sulfur-containing substances in time-dependent manner by the ligand-exchange mechanism connected with the substitution of one diethyldithiocarbamato ligand for one cysteine and/or cystine (CysCys) molecule(s). The results of mass spectrometry and UV/Vis spectroscopy experiments also revealed that the $[Au(dtc)_2]^+$ cations seem to be biologically relevant species influencing the resulting cytotoxicity of the complexes **1–6**, owing to the findings that the complexes **2**, **4** and **6**, having the general composition $[Au(dtc)Cl_2]$, decompose dominantly to a mixture of $[Au(dtc)_2]^+$ and $[AuCl_4]^-$ species in MeOH and DMF solutions.

Acknowledgements

The project was funded by the National Plan for Science and Technology and Innovation (MAARIFAH)-King Abdul Aziz city for Science and Technology-through the Science and Technology unit at King Fahd University of Petroleum and Minerals (KFUPM)-the Kingdom of Saudi Arabia, Award No. 14-MED64-04. The financial support from the National Program of Sustainability I (LO1305) of the Ministry of Education, Youth and Sports of the Czech Republic is gratefully acknowledged.

References

1 N. J. Wheate, S. Walker, G. E. Craig and R. Oun, *Dalton Trans.*, 2010, **39**, 8113.
2 Y. Kidani, M. Noji and T. Tashiro, *Gann*, 1980, **71**, 637.
3 B. Rosenberg, L. van Camp and T. Krigas, *Nature*, 1965, **205**, 698.
4 E. Wong and C. M. Giandomenico, *Chem. Rev.*, 1999, **99**, 2451.
5 V. G. Schweitzer, *Otolaryngol. Clin.*, 1993, **26**, 759.
6 D. J. Stewart, *Crit. Rev. Oncol. Hematol.*, 2007, **63**, 12.
7 S. Dhar and S. J. Lippard, Current Status and Mechanism of Action of Platinum-Based Anticancer Drugs, in *Bioinorganic Medicinal Chemistry*, ed. E. Alessio, Wiley-VCH Verlag GmbH & Co. KGaA, Weinheim, Germany, 2011, p. 79.

8 J. D. S. Chaves, J. L. Damasceno, M. C. F. Paula, P. F. de Oliveira, G. C. Azevedo, R. C. Matos, M. C. S. Lourenço, D. C. Tavares, H. Silva, A. P. S. Fontes, M. V. de Almeida, *Biometals.*, 2015, **28**, 845.

9 T. Gamberi, F. Magherini, T. Fiaschi, I. Landini, L. Massai, E. Valocchia, L. Bianchi, L. Bini, C. Gabbiani, S. Nobili, E. Mini, L. Messori and A. Modesti, *Mol. BioSyst.*, 2015, **11**, 1653.

10 S. S. Al-Jaroudi, M. I. M. Wazeer, A. A. Isab and S. Altuwaijri, *Polyhedron*, 2013, **50**, 434.

11 R. B. Bostancioglu, K. Isik, H. Genc, K. Benkli and A. T. Koparal, *J. Med. Chem.*, 2012, **27**, 458.

12 L. Giovagnini, L. Ronconi, D. Aldinucci, D. Lorenzon, S. Sitran and D. Fregona, *J. Med. Chem.*, 2005, **48**, 1588.

13 A. Casini, M. A. Cinellu, G. Minghetti, C. Gabbiani, M. Coronnello, E. Mini and L. Messori, *J. Med. Chem.*, 2006, **49**, 5524.

14 D. Aldinucci, D. Lorenzon, L. Stefani, L. Giovagnini, A. Colombatti and D. Fregona, *Anti-Cancer Drugs*, 2007, **18**, 323.

15 M. Coronnello, G. Marcon, S. Carotti, B. Caciagli, E. Mini, T. Mazzei, P. Orioli and L. Messori, *Oncol. Res.*, 2001, **12**, 361.

16 M. Monim-ul-Mehboob, M. Altaf, M. Fettouhi, A. A. Isab, M. I. M. Wazeer, M. N. Shaikh and S. Altuwaijri, *Polyhedron*, 2013, **61**, 225.

17 A. Bindoli, M. P. Rigobello, G. Scutari, C. Gabbiani, A. Casini and L. Messori, *Coord. Chem. Rev.*, 2009, **253**, 1692.

18 L. Messori, F. Abbate, G. Marcon, P. Orioli, M. Fontani, E. Mini, T. Mazzei, S. Carotti, T. O'Connell and P. Zanello, *Med. Chem.*, 2000, **43**, 3541.

19 L. Ronconi, L. Giovagnini, C. Marzano, F. Bettio, R. Graziani, G. Pilloni and D. Fregona, *Inorg. Chem.*, 2005, **44**, 1867.

20 V. Milacic, D. Chen, L. Ronconi, K. R. Landis-Piwowar, D. Fregona and Q. P. Dou, *Cancer Res.*, 2006, **66**, 10478.

21 X. Zhang, M. Frezza, V. Milacic, L. Ronconi, Y. Fan, C. Bi, D. Fregona and Q. P. Dou, *J. Cell. Biochem.*, 2010, **109**, 162–172.

22 M. Altaf, M. Monim-ul-Mehboob, A. A. Isab, V. Dhuna, G. Bhatia, K. Dhuna and S. Altuwaijri, *New J. Chem.*, 2015, **39**, 377.

23 E. Barreiro, J. S. Casas, M. D. Couce, A. Sánchez, A. Sánchez-Gonzalez, J. Sordo and E. M. Vázquez-López, *J. Inorg. Biochem.*, 2014, **89**, 138.

24 E. R. Tiekink, *Crit. Rev. Oncol. Hematol.*, 2002, **42**, 225.

25 F. K. Keter, I. A. Guzei, M. Nell, W. E. van Zyl and J. Darkwa, *Inorg. Chem.*, 2014, **53**, 2058.

26 M. Altaf, M. Monim-ul-Mehboob, A. A. A. Seliman, A. A. Isab, V. Dhuna, G. Bhatia and K. Dhuna, *J. Organomet. Chem.*, 2014, **765**, 68.

27 M. Altaf, M. Monim-ul-Mehboob, A. A. A. Seliman, M. Sohail, M. I. M. Wazeer, A. A. Isab, L. Li, V. Dhuna, G. Bhatia and K. Dhuna, *Eur. J. Med. Chem.*, 2015, **95**, 464.

28 M. Altaf, M. Monim-ul-Mehboob, A. A. Isab, V. Dhuna, G. Bhatia, K. Dhuna and S. Altuwaijri, *New J. Chem.*, 2015, **39**, 377.

29 S. S. Al-Jaroudi, M. Monim-ul-Mehboob, M. Altaf, M. Fettouhi, M. I. M. Wazeer, S. Altuwaijri and A. A. Isab, *New J. Chem.*, 2014, **38**, 3199.

30 Stoe & Cie, *X-Area & X-RED32, GmbH*, Darmstadt, Germany, 2009.

31 G. M. Sheldrick, *Acta Crystallogr.*, 2008, **A64**, 112.

32 A. L. Spek, *Acta Crystallogr.*, 2009, **D65**, 148.

33 C. F. Macrae, I. J. Bruno, J. A. Chisholm, P. R. Edgington, P. McCabe, E. Pidcock, L. Rodriguez-Monge, R. Taylor, J. van de Streek and P. A. Wood, *J. Appl. Crystallogr.*, 2008, **41**, 466.

34 A. J. Odola and J. A. O. Woods, *J. Chem. Pharm. Res.*, 2011, **3**, 865.

35 F. Jian, Z. Wang, Z. Bai, X. You, H. Fun, K. Chinnakali and L. A. Razak, *Polyhedron*, 1999, **18**, 3401.

36 A. Jayaraju, M. M. Ahamad, R. M. Rao and J. Sreeramulu, *Pharma Chem.*, 2012, **4**, 1191.

37 J. Chatt, L. A. Duncanson and L. M. Venanzi, *Nature*, 1956, **177**, 1042.

38 C. J. Pouchert, *Aldrich Library of FT-IR Spectra*, Aldrich Chemical Company, Milwaukee, 2nd edn, 1997, vol. 1.

39 C.-M. Che and R. W.-Y. Sun, *Chem. Commun.*, 2011, **47**, 9554.

40 P. Calami, A. Carotti, T. Guerri, L. Messori, E. Mini, P. Orioli, G. P. Speroni and J. Inorg, *Biochem.*, 1997, **66**, 103.

41 R. K. Johnson, C. K. Mirabelli, L. F. Faucette, F. L. McCabe, B. M. Sutton, D. L. Bryan, G. R. Girard and D. T. Hill, *Proc. Am. Assoc. Cancer Res.*, 1985, **26**, 254.

42 C. K. Mirabelli, L. F. Faucette, F. L. McCabe, B. M. Sutton, D. L. Bryan, G. R. Girard, D. T. Hill, J. O. Bartus, S. T. Crooke and R. K. Johnson, *J. Med. Chem.*, 1987, **30**, 2181.

43 L. Ronconi, L. Giovagnini, C. Marzano, F. Bettio, R. Graziani, G. Pilloni and D. Fregona, *Inorg. Chem.*, 2005, **44**, 1867.

44 F. Jian, L. Lu, X. Wang, S. S. Raj, I. A. Razak and H.-K. Fun, *Acta Crystallogr., Sect. C: Cryst. Struct. Commun.*, 2000, **56**, 939.

45 R. V. Parish, B. P. Howe, J. P. Wright, J. Mack, R. G. Pritchard, R. G. Buckley, A. M. Elsome and S. P. Fricker, *Inorg. Chem.*, 1996, **35**, 1659.

46 C. J. L. Lock, M. A. Turner, R. V. Parish and G. Potter, *Acta Crystallogr., Sect. C: Cryst. Struct. Commun.*, 1988, **44**, 2082.

47 G. Mazzone, N. Russo and E. Sicilia, *Organometallics*, 2012, **31**, 3074.

48 T. F. Carlson, W. H. Watson, Private communication to the Cambridge Structural Database, deposition number CCDC 160743.†

49 J. Vicente, M.-T. Chicote, P. Gonzalez-Herrero and P. G. Jones, *Inorg. Chem.*, 1997, **36**, 5735.

50 D. Jentsch, P. G. Jones, C. Thone and E. J. Schwarzmann, *J. Chem. Soc., Chem. Commun.*, 1989, 1495.

51 J. Vicente, M. T. Chicote, P. Gonzalez-Herrero, P. G. Jones, M. G. Humphrey, M. P. Cifuentes, M. Samoc and B. Luther-Davies, *Inorg. Chem.*, 1999, **38**, 5018.

52 D. Saggioro, M. P. Rigobello, L. Paloschi, A. Folda, S. A. Moggach, S. Parsons, L. Ronconi, D. Fregona and A. Bindoli, *Chem. Biol.*, 2007, **14**, 1128.

53 C. F. Shaw, M. T. Coffer, J. Klingbeil and C. K. Mirabelli, *J. Am. Chem. Soc.*, 1988, **110**, 729.

54 G. Salemi, M. C. Gueli, M. D'Amelio, V. Saia, P. Mangiapane, P. Aridon, P. Ragonese and I. Lupo, *J. Neurol. Sci.*, 2009, **30**, 361.